Stability analysis and design of cemented backfill wall for underground hard-rock mines using numerical modelling

Ashok Kumar Godugu[1], Sreenath Sekhar[2], John Loui Porathur[2,*] and Shubham Bhargava[2]

[1]Hindustan Zinc Limited, Dariba, Rajsamand 313 211, India
[2]CSIR-Central Institute of Mining and Fuel Research, Nagpur Research Centre, 17/C, Telankhedi, Civil Lines, Nagpur 440 001, India

A methodology using three-dimensional elasto-plastic analysis has been formulated to assess the required strength parameters for a stable backfill wall for various dimensions of a stope. The numerical modelling results show linearly increasing trend for the required backfill cohesion with respect to stope height for longer stopes and curvilinear with flattening trend for shorter stopes. Comparison of the numerical modelling results with those of a popular theoretical equation shows that the theoretical equation fails to represent the interface friction and tension. The numerical modelling methodology is a better tool which can capture a gamut of aspects. The developed methodology has been used to estimate the required pastefill strength and binder percentage for a hard rock mine in North India, where it has been successfully implemented in over 50 stopes without any significant case of backfill failure.

Keywords: Elasto-plastic analysis, field implementation, hard-rock mining, numerical modelling, pastefill.

BACKFILLING of underground stopes using cemented paste or hydraulic fill is gaining popularity and is a well-established technology now[1,2]. Earlier underground mining was done mainly using open stoping methods by leaving considerable amounts of ore, to the tune of about 25–30%, in support pillars. Due to scarcity of metalliferous ore, to improve ground stability and ore recovery, most of the mines have switched to backfilling methods. Backfilling of the stopes is effective as it provides a confinement to the walls around the voids and prevents them from failing, giving a regional stability and control subsidence[3]. It also reduces relaxation of the surrounding rock mass and thereby allows the rock to bear the load[4]. Backfilling increases the ore recovery by reducing pillar volume and facilitates a safe disposal of the solid waste generated in an eco-friendly manner[5,6]. The stability of the fill mass is a function of the type of filling material, method of filling, dimension of the exposed fill, and degree of stress arching and confinement[7]. Cemented backfilling methods currently in practice include cemented hydraulic fill, cemented rock fill and cemented pastefill. Among these, cemented pastefill is the trending technology suited for high-production mining. The pastefill is composed of about 80–85% solid material by mass and 15–20% water. It is emplaced into stopes through pipelines and boreholes[8]. The solids include sand, screened mill tailings or aggregates and a binder which is usually ordinary Portland cement (OPC). The binder percentage is a major factor that determines the gain in strength of the pastefill. Cement in the pastefill absorbs most of the water in it during the curing process[9]. The cement content generally used in backfills is about 1–10% by weight of solids.

In high-production mining methods such as blast hole stoping, alternate primary and secondary stopes are demarcated. The primary stopes are extracted first and backfilled. The backfill is allowed to cure for a period of time. The secondary stopes are then extracted. The side wall of the filled primary stope will be exposed during secondary stope extraction. Any failure of the backfilled material from the primary stope may result in ore dilution and even lead to ground instability. Thus, stability of backfill walls is of paramount importance. Designing of the pastefill material must consider the change in stress in the backfill material and the rock mass around the stope[10]. Several researchers in the past have proposed theoretical and numerical methods for predicting stability of the pastefill so as to present the required strength for a cemented backfill material. Mitchell *et al.*[11] had proposed a theoretical equation (eq. (1)) to derive the required engineering properties of the cemented backfill, based on stope dimensions. Their equation for evaluating the factor of safety of a fill wall is widely used and is applicable for those stopes with width considerably lower than their height.

$$F = \frac{\tan\phi}{\tan\alpha} + \frac{2cLw}{wH*(\gamma L - c_b)\sin 2\alpha}, \quad (1)$$

where F is the factor of safety of the backfill wall, ϕ the friction angle of the cemented backfill, α the angle that the critical plane makes with the horizontal, c the cohesion of

*For correspondence. (e-mail: johnlouip@gmail.com)

the cemented backfill, L the stope length, w the stope width, h the stope height, γ the effective unit weight of cemented backfill and c_b is the interface cohesion.

Similar studies based on the stability of the backfill materials were done by various researchers. The estimation of stress distribution in the backfill has been done based on the two-dimensional plane-strain theory proposed by Marston[12] and later modified by others[13–15]. From the literature review, it is evident that the stability of pastefill stopes increases with an increase in binder percentage and decreases with increase in stope dimension[7,16–18]. The three-dimensional wedge model based on limit equilibrium method by Mitchell *et al.*[11] has been subjected to modification by several authors[19–23]. The equation proposed by Mitchell *et al.*[11] has been modified by Yang and Li[24] by incorporating a surcharge, various stope ratios and lower cohesion along the side walls. They had also used numerical modelling to validate their modification.

The wedge failure theory presented by Mitchell *et al.*[11] and the modification presented by Yang and Li[24] have several limitations. The stress development in the pastefill due to the confining rock walls and frictional resistance at fill–rock interface is ignored in the theoretical model. The phenomenon of stress arching, by which the vertical stress acting in the bottom portion of the pastefill column is considerably lower than the theoretical cover pressure[25], has not been captured in their theoretical treatment. The stress measurement conducted at mine sites by various researchers is in favour of the stress arching phenomenon[26–31]. Hence the shear strength requirement predicted using theoretical equations may be higher. Though the binder content in the fill mix increases its strength, it increases the overall cost of backfilling. Hence it is important to estimate the optimum binder content in the backfill mix. Researchers in the past have attempted numerical modelling for verification of the theoretical models[24,32]; however, the fill mix design had essentially been carried out using the theoretical equations. Numerical modelling is a far more versatile tool to predict ground behaviour with its capability to capture a gamut of aspects such as stress distribution, geometrical complexities and surrounding rock-mass behaviour on the fill mass.

In this study, a three-dimensional numerical modelling approach is used to assess the stability of a free-standing, cemented, backfill wall. The study was conducted based on a case example from an underground hard-rock mine located in North India. The stoping parameters used in numerical modelling were those matching with the case example. Laboratory testing of the pastefill samples was done to provide inputs to the numerical modelling.

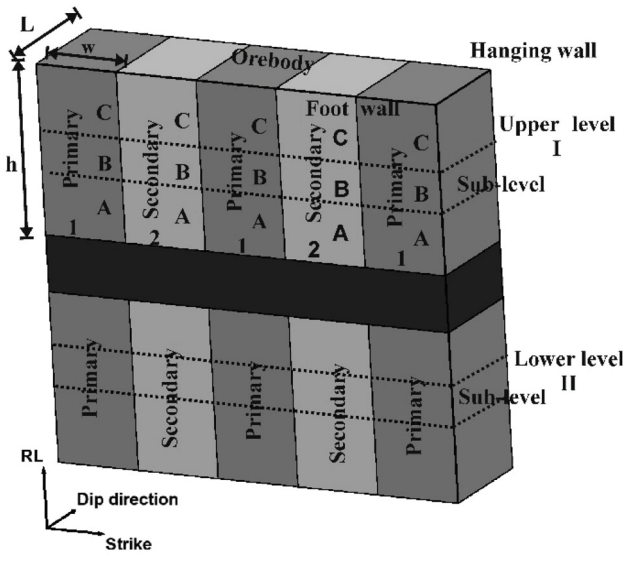

Figure 1. Schematic representation of primary and secondary mining.

Case example of a lead–zinc–silver mine

The case example presented here is that of a lead–zinc–silver mine with a competent rock mass, mostly composed of dolomite and graphite mica schist. Cemented pastefill wall stability was studied with an aim to implement at this site. The rock mass rating (RMR) of the rock mass varied between 60 and 75 and fell in the 'good' category[33]. The orebody was steeply dipping with gradient between 70° and 90°, and had a width ranging from 10 to 80 m. The level interval varied between 60 and 100 m. Blast hole stoping was done with cemented hydraulic fill or cemented paste backfill in the primary and secondary sequence. The mine currently operates at a depth range 100–600 m from the surface. Most of the stopes are transverse in configuration and only a few are longitudinal, where the orebody has narrowed to 10–15 m. Figure 1 is a schematic diagram showing the mining sequence. The general sequence of mining is from top to bottom by leaving a sill pillar after each level (I and II in Figure 1). In one stoping level, a stope will have a height h and is divided into alternate primary (i) and secondary (ii) stopes of width w. The length of each stope (L) varies based on the width of the orebody (hanging wall to footwall distance) in that region. Individual stopes may be extracted in sub-levels with a bottom-to-top sequence by backfilling (A–C in Figure 1). Depending on the rock-mass competency and presence of major planes of weakness, the height of the pastefill wall exposure is decided for individual stopes. In a highly competent rock mass, a stope height of even 100 m can be extracted with backfilling the full height after extraction of all sub-levels. Whenever the rock mass is slightly weaker with the presence of shear planes or fault planes the stopes are extracted and backfilled in sub-levels, proceeding from the bottom to the top. The sub-level interval ranged between 25 and 50 m. Sometimes two sub-levels may be extracted

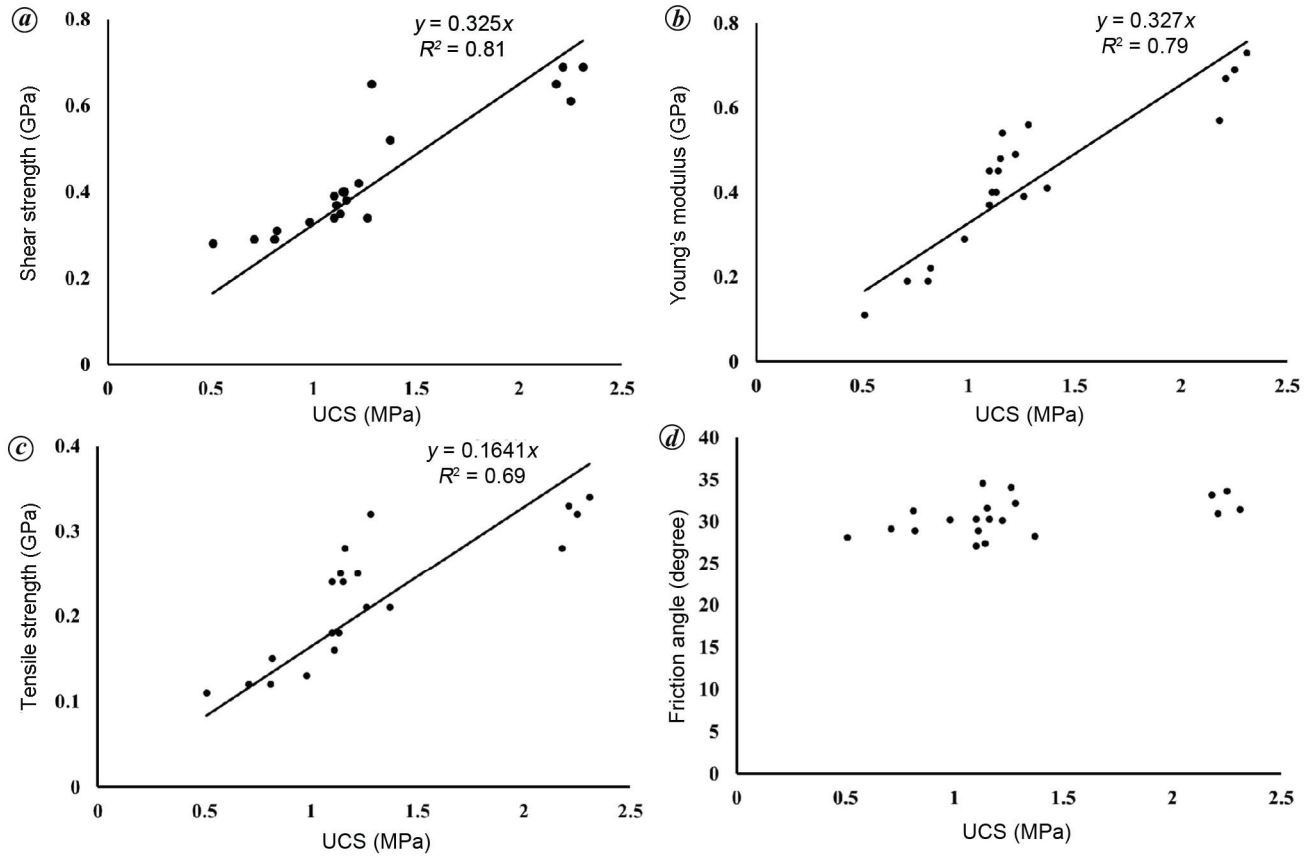

Figure 2. Relationship of various parameters, viz. (***a***) shear strength, (***b***) Young's modulus, (***c***) tensile strength and (***d***) friction angle, with respect to uniaxial compressive strength (UCS).

and backfilled together depending upon the rock mass quality in that region. Similar sequence is followed in primary as well as secondary stoping. During secondary stoping, the backfill wall of the adjacent primary stopes will be exposed. The free-standing backfill wall height in this mine can therefore be in the range 25–100 m. Stope width w of transverse stopes varies between 25 and 35 m and the length varies between 10 and 80 m depending on the width of orebody in each stope block. The mine currently has provisions for using cemented hydraulic fill as well as cemented pastefill, but it will be adopting cemented pastefill for all the future stoping areas.

Strength of cemented pastefill

Mill tailings and the binder, OPC, from the mine site were brought to the laboratory. Cemented pastefills of various percentages of binder weight with respect to the total solid weight were prepared in the laboratory. The binder percentage used was 4, 5, 6, 7 and 8 with corresponding percentage of mill tailings of 96, 95, 94, 93 and 92 respectively. The samples were cured for 7, 14, 28 and 56 days, and tested for their engineering properties such as uniaxial compressive strength (UCS), Young's modulus, cohesion, angle of internal friction and tensile strength. The tests conducted included uniaxial compression test, triaxial compression test and Brazilian tensile strength test. UCS is a standard strength parameter and is easy to determine. It is not practical to conduct all the above tests to determine the engineering properties needed for numerical simulation on a day-to-day basis. Hence correlations were made for the required strength parameters and elastic constants with respect to UCS. Linear best-fit curves were obtained for shear strength, Young's modulus, tensile strength and friction angle with respect to UCS of all the samples tested (Figure 2 *a–d*).

The linear best-fit curves passing the origin were drawn, which yielded correlation coefficient in the range 0.69–0.81 (Figure 2 *a–c*). The angle of internal friction did not exhibit any particular trend with respect to age or binder percentage or UCS of pastefill and had an average value of 30.5° with a standard deviation of 2.18° (Figure 2 *c*). *In situ* core samples were extracted and tested for UCS from backfilled stopes of various ages and binder percentages. It has been observed that UCS obtained from *in situ* samples was about 20–25% lower than that of the laboratory-prepared samples of the same composition and age. This aspect, as well as other uncertainties, such as

cold joints formation during filling stoppages, possible error in binder percentage in the mix and dynamic loading were accounted for using a factor of safety during field applications. Figure 3 shows the variation of UCS with respect to binder percentage. The trend shows that the binder percentage in the fill mix greatly improves its strength, especially after 28 days of curing.

Numerical modelling

A steeply dipping orebody was modelled using a well-known three-dimensional finite-difference software. The model was truncated using a vertical plane of symmetry passing through the centre of the orebody and across the stope length (L; Figure 4). Mohr–Coulomb elasto-plastic analysis was performed to assess the stability of the pastefill and the surrounding rock mass. A typical blast-hole stoping using primary and secondary stoping sequences was simulated in stages. The stope dimensions were varied to get a range of practical stope sizes used in the case example. The stope heights simulated were 25, 35, 60, 75 and 100 m, the stope length varied from 10 m for a longitudinal stope, to 30, 45, 60 and 80 m for transverse stopes. The stope length is denoted here as the hanging wall to footwall distance of a stope. As there is not much variation, the width of the stope was kept constant at 30 m for all the models. It is experienced in the field that while backfilling of a stope, the fill does not reach till the top of the stope void and the backfill also settles after some time. This will result in a small gap at the roof of the stope. To account for this in the numerical models, a gap of 1 m was left between the fill top and the stope back (Figure 4). The same strategy has been applied earlier by various researchers in their numerical modelling attempts[25,34]. Fill–rock interface was simulated at the hanging wall contact, stope bottom and adjacent stope contact (Figure 4).

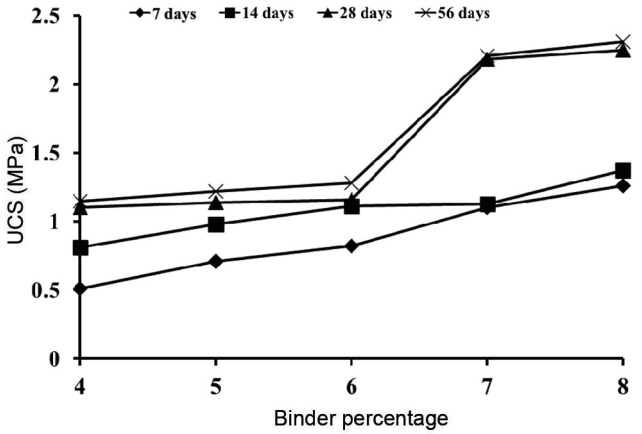

Figure 3. Variation of UCS with respect to binder percentage.

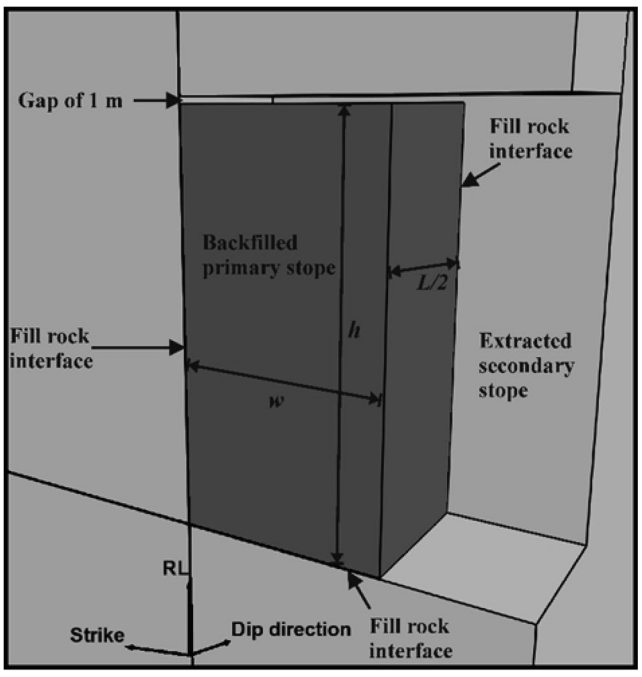

Figure 4. Three-dimensional model.

Method to determine the fill-wall strength

Laboratory analyses have already revealed that the friction angle of the pastefill does not vary significantly with the variation in other engineering properties such as UCS, cohesion and Young's modulus. Based on the literature review, it was found that the researchers used the same values for the interface friction angle and internal friction angle of the backfill[13]. According to Marston[12], the interface friction angle lies between one-third and two-thirds of the internal friction angle of the fill material. Experimental studies using artificial cemented backfill reveal that the interface friction angle can be greater than two-thirds the internal friction angle of the paste backfill[35,36]. Hence in this study, the internal friction angle of the pastefill was kept constant at 30° and the rock–pastefill interface friction angle was kept constant at two-thirds of the pastefill internal friction angle, that is, 20° (refs 21 and 25). Several published works indicate that the backfill–interface cohesion is lower than the pastefill cohesion[37]. A series of direct shear stress tests conducted by Koupouli *et al.*[38] showed the interface cohesion c_b is about 0.5–0.6 times that of the backfill cohesion. Parametric studies by Li and Aubertin[21] indicated that when the interface cohesion is about 25% of the cemented backfill, stress analysis of a backfill system produced the best-fitting situation. The interface cohesion and friction angle are also dependent on rock-wall roughness. To be on the safer side and in the absence of site measurement, the interface cohesion was taken as 25% of the fill for all the models. The other parameters

such as tensile strength, shear strength (cohesion) and the interface cohesion were varied proportionately to the corresponding UCS to achieve the limiting state of failure of the fill mass (Figure 2 *a–c*). Researchers have earlier found that the displacement magnitude is a good indicator of failure manifestation in elasto-plastic analysis[24,32,39]. A similar approach has been used here coupled with plasticity indicator of the zones for estimation of the critical state of a pastefill wall. Displacement histories were plotted while equilibrating the models for a set of strength parameters applied to the pastefill. The strength of the pastefill was reduced after equilibrating the model by a small value (corresponding to about 5 kPa of its UCS), and the model was again run for a fixed number of steps. While reducing the strength parameters, friction angle was omitted as it did not show any variation with respect to UCS; only cohesion, interface cohesion and tensile strength were considered. Figure 5 reveals that when the model is in a stable state, the displacement at the face of the pastefill tends to stabilize. When the model reaches an unstable state, the displacement will continuously and steeply increase. At the same time, a wedge-shaped failure zone can be observed developing approximately along the critical angle α which connects the toe of the fill wall to either the rock–fill interface wall or to the top surface of the fill (Figure 5). The critical angle α has been calculated in all the models which approximately ranged between 55° and 60°; this is in corroboration with the critical angle ($\alpha = 45° + \phi/2$) obtained from the Mohr–Coulomb theory. This concept was also used by Mitchell *et al.*[11] in their wedge failure theory of a backfill wall. After several hit and miss attempts, the strength reduction increment and the number of solution cycles were determined to evaluate the pastefill wall strength to a reasonable accuracy. The minimum strength factor (SF) resulting in a stable state of the fill mass was then estimated from the model (Figure 5). The required UCS of the pastefill is $500 \times \text{SF}$ in kPa. The corresponding required cohesion, Young's modulus and tensile strength can be estimated from Figure 2 *a–c* respectively.

The stope dimensions were varied as mentioned above and for each combination of h and L, the minimum backfill strength resulting in a stable wall was estimated from numerical modelling. Figure 6 presents the variation of required backfill strength in terms of its cohesion and the corresponding UCS with respect to the stope height. From the figure, it can be seen that the requirement of backfill strength increases almost linearly with respect to the fill height for longer stopes and increases curvilinearly with flattening trend for shorter stopes. It is also evident that when the distance between the footwall and hanging wall (L) reduces, the stability of the fill wall increases considerably due to stress arching. This aspect of stress arching and associated friction at the wall contact has been captured in numerical modelling, which was ignored in the earlier theoretical models. When the stope length is higher, the effect of wall friction will be lower, which results in a linear trend with respect to the fill height. The fill wall stability is more sensitive towards the fill height compared to the stope length. The effect of stope length can be clearly seen in the minimum stable backfill strength versus stope length plot (Figure 7). Curvilinear graphs with flattening trend can be observed with respect to increase in stope length for all stope heights. The required cohesion obtained using the theoretical equation of Mitchell *et al.*[11] (eq. (1)) was compared with that of the numerical modelling result (Figure 7). From Figure 7 it can be seen that Mitchell *et al.*[11] (eq. (1)) clearly overestimate the required backfill strength requirement. Further, the theoretical curves do not indicate the anticipated drop in the required cohesion at lower stope length. This is due to the fact that the stress arching and friction at the rock–fill interface is ignored in the theoretical equation proposed by Mitchell *et al.*[11]. Numerical modelling is a

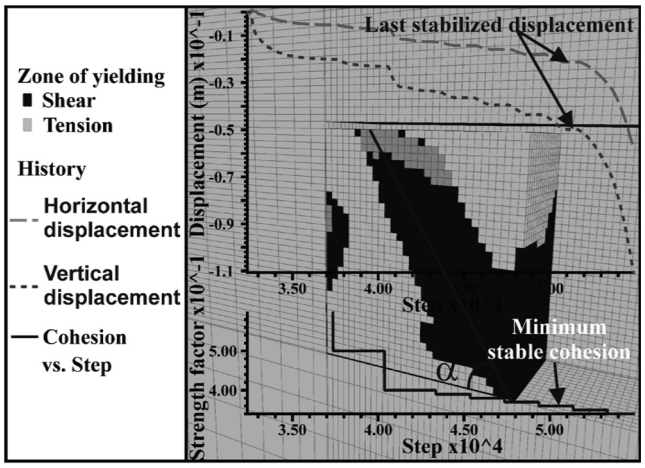

Figure 5. Method to determine fill wall stability from yielded zones and history of displacements.

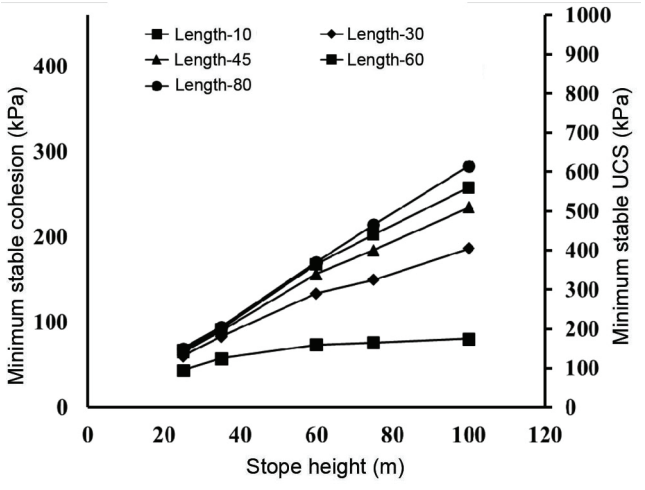

Figure 6. Variation in minimum stable cohesion and UCS with respect to stope height.

far more superior tool compared to the simplified theoretical models.

Numerical modelling results from Figures 6 and 7 were now used as nomograms to arrive at the required strength of the cemented pastefill wall depending on stope length (L) and height of exposure (h). Stability of the pastefill wall is needed only in the short term, say, for a month or two. However, a safety factor of 1.5 is recommended for site implementation to account for backfill strength reduction under *in situ* condition, possible error in cement percentage in the fill mix, stoppages during the backfilling process resulting in cold joints and planes of weakness, and dynamic stress acting on the pastefill wall due to blast vibrations. The factor of safety is subjective and should be decided for each mine site considering the above factors and confidence level of the mine management. Hence the required strength of the backfill is as follows:

$$\text{UCS required} = \text{FoS} \times \text{minimum UCS resulting in stable fill wall}, \quad (2)$$

where FoS is the factor of safety, which is taken as 1.5 for this particular case example.

The binder percentage required to achieve the above strength can be estimated from Figure 3 for each stope depending on the age of the backfill of the adjacent primary stope.

From numerical modelling, the modes of backfill mass failure were analysed. The primary modes of failure in all cases were shear failure along the critical plane. At the same time, separation or slippage was also observed along with the rock–fill interfaces. Tensile separation at the upper portion of the rock–fill interface could be seen for stopes of greater height and shear slippage was observed at the lower region. The aspect of tensile failure has not been addressed in any of the theoretical models proposed earlier. The numerical modelling result shows that the tensile stress which builds up at the top portion of the rock–fill interface cannot be ignored and may play a significant role in the overall stability of the backfill. At the same time, 'stress arching' at the lower portion will provide frictional resistance. Numerical modelling is therefore a more versatile tool and will have greater relevance to optimally design pastefill mix.

Field implementation

When the stoping and its backfilling are done to their full height, the maximum height of the pastefill height can go up to 100 m for this mine site. When they are extracted and backfilled in sub-levels, the exposed wall height may be in the range 25–60 m. However, for lower sub-levels the pastefill wall, though not exposed to full height, may experience vertical surcharge loading from the upper sub-levels. Hence the required strength of pastefill for sub-level-wise backfilling will be applicable only for the top sub-level. For the bottom and middle sub-levels, it will be prudent to estimate the height from the toe to the top level. The required UCS along with the corresponding shear strength, Young's modulus and tensile strength of the backfill material has been obtained from the correlation graphs in Figure 2 *a–c* and presented in Table 1 for various fill heights and stope lengths. From the table, it is clear that even for the maximum height (100 m) and maximum length (80 m) of the pastefill wall applicable to the case example, the required UCS does not exceed 1 MPa. From the laboratory-tested values of UCS versus binder percentage (Figure 3), it can be ascertained that the binder percentage requirement is not more than 4 at the mine site for a minimum 28 days cured pastefill. At lower binder percentage there is a risk of fill liquefaction[40], which may result in breach of the bulkhead and flooding of the workings. The binder is the main ingredient that absorbs the water content in the backfill pulp, which enables proper curing. Hence it is not prudent to use lower binder content in the backfill mix until the liquefaction potential has been further studied in detail, which is beyond the scope of this study. The mine practices backfilling of a stope void in two stages: 7 m height of plug fill is formed first with higher binder content and cured for 7 days, followed by the bulk fill of the remaining void with lower binder content. Though the use of more than 4% binder content may not be required at this particular mine site for any possible stope dimensions, 5% or 6% OPC may be used in the plug portion to ensure faster curing and better

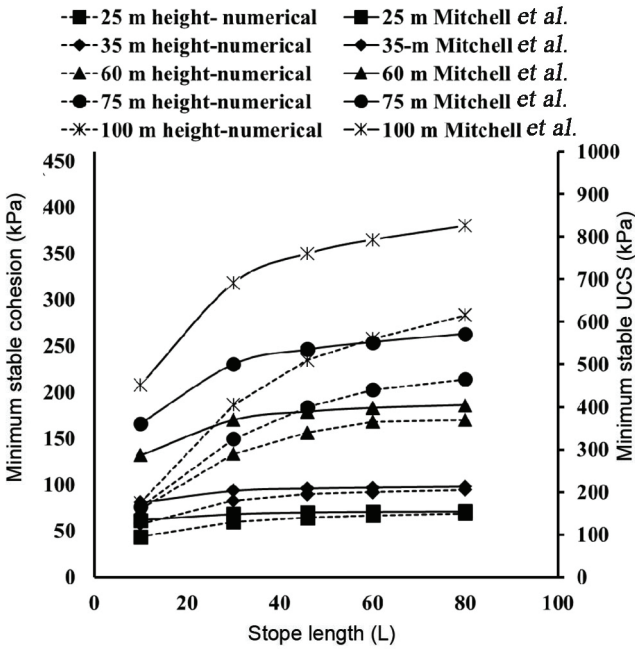

Figure 7. Variation in minimum stable cohesion and UCS with respect to stope length.

Table 1. Summary of required strength parameters for various stope dimensions

Height (m)	Length (m)	Uniaxial compressive strength (kPa)	Cohesion (kPa)	Tensile strength (kPa)	Young's modulus (MPa)
100	10–80	262.5–922.5	120.75–424.35	43–151.38	85.83–301.66
75	10–80	247.5–697.5	113.85–320.85	40.61–114.46	80.93–228
60	10–80	240–555	110.4–320.85	39.38–91	78.48–181.48
35	10–80	187.5–307.5	86.25–141.45	30.76–50.46	61.31–100.55
25	10–80	195–225	65.5–103.5	23.38–36.92	46.59–73.57

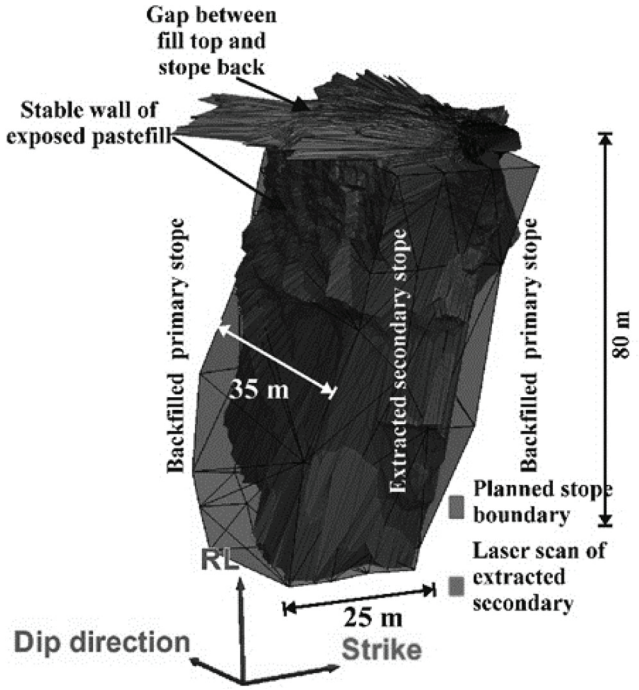

Figure 8. Laser scan image of a secondary stope with stable pastefill wall on both sides.

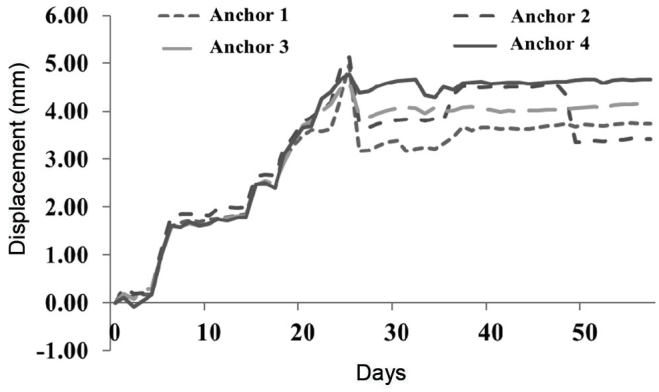

Figure 9. Footwall ground movement observed from a multi-point borehole extensometer.

safety against barricade failure. The bulk fill will require only 4% OPC. The mine has practised cemented paste backfill in over 50 stopes without any case of pastefill wall failure reported so far, other than some minor spalling observed during blasting. Figure 8 shows a cavity monitoring system (CMS) laser scan image of a blasted secondary stope with fill wall exposure of the adjacent primary stope at the mine site. The laser scan indicates practically no over-breakage of the fill wall on either side of the secondary stopes. Further, the gap formed over

primary as well as secondary stopes at the top portion has been captured in the CMS scan image. Rock mass movement of the footwall has been monitored using multipoint borehole extensometer (MPBX; Figure 9). The instrument indicated slight rise in the displacement (maximum about 5 mm) of the footwall during excavation, which soon stabilized after backfilling of the voids. It was observed that with paste backfilling, the overall surrounding rock mass stability and ore recovery had improved considerably.

Scope for future work

The numerical model presented here was implemented for a particular mine site. To make the numerical modelling approach more versatile, some more parameters such as orebody inclination and stope width may be included. The effect of rock-mass surface roughness and rock–fill interface properties has to be analysed in detail. Dynamic loading due to blasting and its effects on the fill wall stability is another area which requires attention.

Conclusion

In this study, a methodology for assessing the stability of a cemented backfill wall using three-dimensional numerical modelling with Mohr–Coulomb elasto-plastic analysis has been developed. The method essentially involves a displacement tracking system at the backfill wall and pattern of yielding before and after backfill failure. It enables the user to determine the minimum required strength parameters such as UCS, cohesion and tensile strength for a stable backfill wall using 3D numerical modelling. From the laboratory testing of pastefill specimens, correlation graphs with linear best-fit relation have been drawn for inter-relation between various strength parameters. However, those correlations are particular to the mine site under study and may not be directly applicable to other sites. From the numerical modelling conducted using the above methodology, the effect of stope dimensions such as stope height and stope length was studied, which was according to the anticipated trend. Numerical results have been compared with a theoretical equation[11]. The comparison proved that the theoretical equation was actually insufficient to capture various aspects of stress build-up in the fill mass and rock–fill interaction, and hence overestimated the required cohesion. It is always prudent to adopt numerical modelling techniques such as the one presented here to obtain optimum fill design. Numerical modelling has been found to capture a wider range of aspects that can directly or indirectly affect the backfill wall stability. From the modelling results, an optimum pastefill composition has been recommended at the mine site under study, which has been successfully implemented. The numerical modelling approach (depicted here), for the estimation of cemented backfill wall stability, can be applied to similar mine sites.

1. Potvin, Y., Thomas, E. and Fourie, A., *Handbook on Mine Fill*, Australian Centre for Geomechanics, 2005, p. 179.
2. Belem, T. and Benzaazoua, M., Design and application of underground mine paste backfill technology. *Geotech. Geol. Eng*., 2008, **26**(2), 147–174.
3. Brady, B. H. G. and Brown, E. T., *Rock Mechanics for Underground Mining: Third Edition*, 2004; doi:10.1007/978-1-4020-2116-9.
4. Grice, A., Underground mining with backfills. In Proceedings of the Second Annual Summit – Mine Tailings Disposal Systems, Brisbane, Australia, 1998.
5. Sivakugan, N., Veenstra, R. and Naguleswaran, N., Underground mine backfilling in Australia using paste fills and hydraulic fills. *Int. J. Geosynth. Ground Eng*., 2015, **1**(2); doi:10.1007/s40891-015-0020-8.
6. Sivakugan, N., Rankine, K. and Rankine, R., Permeability of hydraulic fills and barricade bricks. *Geotech. Geol. Eng*., 2006, **24**(3), 661–673; doi:10.1007/s10706-005-2132-8.
7. Bloss, M. L., *Prediction of Cemented Rock Fill Stability: Design Procedures and Modelling Techniques*, Ph.D. thesis, University of Queensland, 1992.
8. Landriault, D. and Goard, B., Research into high-density backfill placement methods by the Ontario Division of INCO-Limited. *CIM Bull*., 1987, **80**(897), 46–50.
9. Villaescusa, E., Mine fill. In *Geotechnical Design for Sublevel Open Stoping*, CRC Press, Boca Raton, Florida, USA, 2014, pp. 405–434.
10. Pirapakaran, K. and Sivakugan, N., Arching within hydraulic fill stopes. *Geotech. Geol. Eng.*, 2007, **25**(1), 25–35.
11. Mitchell, R. J., Olsen, R. S. and Smith, J. D., Model studies on cemented tailings used in mine backfill. *Can. Geotech. J*., 1982, **19**(1), 14–28; doi:10.1139/t82-002.
12. Marston, A., The theory of external loads on closed conduits in the light of the latest experiments. In Proceedings of Highway Research Board, 1930, vol. 9.
13. Terzaghi, K., Bearing capacity. *Theor. Soil Mech.*, 1943, 118–143.
14. Terzaghi, K., Peck, R. B. and Mesri, G., *Soil Mechanics in Engineering Practice*, John Wiley, New York, USA, 1996.
15. Aubertin, M., Li, L., Arnoldi, S., Belem, T., Bussière, B., Benzaazoua, M. and Simon, R., Interaction between backfill and rock mass in narrow stopes. *Soil Rock Am*., 2003, **1**, 1157–1164.
16. Bloss, M. L. and Chen, J., Drainage research at Mount Isa Mines Limited 1992–1997. In Proceedings of the Sixth International Symposium on Mining with Backfill: Minefill, AusIMM, Brisbane, Australia, 1998, vol. 98, pp. 111–116.
17. Bloss, M. L. and Revell, M. B., Mining with paste fill at BHP Cannington. In Proceedings of The International Symposium on Mining with Backfill, Colorado, Canada, 2001, pp. 209–221.
18. Jewell, R. J. and Fourie, A. B., *Paste and Thickened Tailings – A Guide*, Australian Centre for Geomechanics, The University of Western Australia, 2006.
19. Zou, S. and Nadarajah, N., Optimizing backfill design for ground support and cost saving. In Proceedings of Golden Rocks 2006, The 41st US Symposium on Rock Mechanics, American Rock Mechanics Association, 2006.
20. Dirige, A. P. E., McNearny, R. L. and Thompson, D. S., The effect of stope inclination and wall rock roughness on back-fill free face stability. In Proceedings of Rock Engineering in Difficult Conditions: The Third Canada–US Rock Mechanics Symposium, Toronto, 2009, pp. 9–15.
21. Li, L. and Aubertin, M., An improved method to assess the required strength of cemented backfill in underground stopes with an open face. *Int. J. Min. Sci. Technol*., 2014, **24**(4), 549–558.

22. Li, L. and Aubertin, M., A modified solution to assess the required strength of exposed backfill in mine stopes. *Can. Geotech. J.*, 2012, **49**(8), 994–1002.
23. Li, L., Generalized solution for mining backfill design. *Int. J. Geomech.*, 2014, **14**(3).
24. Yang, P. Y. and Li, L., Numerical and limit equilibrium stability analyses of cemented mine backfill upon vertical exposure. In UMT 2017: Proceedings of the First International Conference on Underground Mining Technology (eds Hudyma. M. and Potvin, Y.), Australian Centre for Geomechanics, Perth, 2017, pp. 399–408.
25. Liu, G., Li, L., Yang, X. and Guo, L., Numerical analysis of stress distribution in backfilled stopes considering interfaces between the backfill and rock walls. *Int. J. Geomech.*, 2017, **17**(2); doi:10.1061/(ASCE)GM.1943-5622.0000702.
26. Askew, J., McCarthy, P. L. and Fitzgerald, D. J., Backfill research for pillar extraction at ZC/NBHC. In Proceedings of 12th Canadian Rock Mechanics Symposium, Canadian Institute of Mining and Metallurgy, Sudbury, Ontario, 1978, pp. 100–110.
27. Knutsson, S., Stresses in the hydraulic backfill from analytical calculations and *in situ* measurements. In Proceedings of Conference on the Application of Rock Mechanics to Cut and Fill Mining, 01/06/1980-03/06/1980, The Institution of Mining and Metallurgy, London, 1981, pp. 261–268.
28. Belem, T., Harvey, A., Simon, R. and Aubertin, M., Measurement and prediction of internal stresses in an underground opening during its filling with cemented fill. In Proceedings of the Fifth International Symposium on Ground Support in Mining and Underground Construction (eds Villaescusa and Potvin), Perth, Western Australia, Australia, 2004, pp. 619–630.
29. le Roux, K., Bawden, W. F. and Grabinsky, M. F., Field properties of cemented paste backfill at the Golden Giant mine. *Min. Technol.*, 2005, **114**(2), 65–80.
30. Grabinsky, M. W. and Bawden, W. F., *In situ* measurements for geomechanical design of cemented paste backfill systems. In Proceedings of the Ninth International Symposium in Mining with Backfill, Montréal, Quebec, Canada, 2007, vol. 29.
31. Thompson, B. D., Bawden, W. and Grabinsky, M. W., *In situ* measurements of cemented paste backfill at the Cayeli Mine. *Can. Geotech. J.*, 2012, **49**(7), 755–772.
32. Liu, G., Li, L., Yang, X. and Guo, L., Required strength estimation of a cemented backfill with the front wall exposed and back wall pressured. *Int. J. Min. Miner. Eng.*, 2018, **9**(1), 1–20; doi:10.1504/IJMME.2018.091214.
33. Bieniawski, Z. T., Rock mass classifications in rock engineering. In Proceedings of the Symposium on Exploration for Rock Engineering, A. A. Balkema, Cape Town, 1976, vol. 1, pp. 97–106.
34. Yu, Q., Chen, X., Dai, Z., Nei, L. and Soltanian, M. R., Numerical investigation of stress distributions in stope backfills. *Period. Polytech. Civ. Eng.*, 2018, **62**(2), 533–538; doi:10.3311/PPci.11295.
35. Nasir, O. and Fall, M., Shear behaviour of cemented pastefill-rock interfaces. *Eng. Geol.*, 2008, **101**(3–4), 146–153.
36. Fall, M. and Nasir, O., Mechanical behaviour of the interface between cemented tailings backfill and retaining structures under shear loads. *Geotech. Geol. Eng.*, 2010, **28**(6), 779–790.
37. Koupouli, N. J. F., Belem, T. and Rivard, P. Shear strength between cemented paste backfill and natural rock surface replicas. In UMT 2017: Proceedings of the First International Conference on Underground Mining Technology (eds Hudyma, M. and Potvin, Y.), Australian Centre for Geomechanics, Perth, 2017, pp. 375–385; https://doi.org/10.36487/ACG_rep/1710_29_Koupouli
38. Koupouli, N. J. F., Belem, T., Rivard, P. and Effenguet, H., Direct shear tests on cemented paste backfill–rock wall and cemented paste backfill–backfill interfaces. *J. Rock Mech. Geotech. Eng.*, 2016, **8**(4), 472–479; doi:10.1016/j.jrmge.2016.02.001.
39. Porathur, J. L., Jose, M., Bhattacharjee, R. and Tewari, S., Numerical modelling approach for design of water-retaining dams in underground hard rock mines – a case example. *Arab. J. Geosci.*, 2018, **11**(23), 750.
40. Clough, G. W., Iwabuchi, J., Rad, N. S. and Kuppusamy, T., Influence of cementation on liquefaction of sands. *J. Geotech. Eng.*, 1989, **115**(8), 1102–1117.

ACKNOWLEDGEMENTS. We thank the Director, CSIR-Central Institute of Mining and Fuel Research (CIMFR), Nagpur and the Director, Indian Institute of Technology (Indian School of Mines), Dhanbad for permission to publish this work. We also thank the scientists and staff of the Mine Backfilling Department of CSIR-CIMFR for laboratory testing, and the officers of Hindusthan Zinc Limited, Rajsamand for help during field implementation. The views expressed are those of the authors and not necessarily of the institutions to which they belong.

Received 3 November 2020; accepted 28 July 2021

doi: 10.18520/cs/v121/i7/920-928